A MAGNETIC BUMPER-TETHER SYSTEM USING ZFC Y123

Roy Weinstein, Drew Parks and Ravi-Persad Sawh
Institute for Beam Particle Dynamics and
Texas Center for Superconductivity
University of Houston
Houston, Texas

Victor Obot and Jianxiong Liu
Dept. of Mathematics
Texas Southern University
Houston, Texas

G. D. Arndt
NASA Johnson Space Center
Houston, Texas

SUMMARY

We consider the use of magnetic forces in a bumper system, to soften docking procedures. We investigate a system which exhibits no magnetic field except during the docking process, which, if desired, can automatically tether two craft together, and which provides lateral stability during docking. A system composed of zero field cooled $Y_{1.7}Ba_2Cu_3O_{7-\delta}$ (Y123) tiles and electromagnets is proposed. The Y123 high temperature superconductor (HTS) is mounted on one craft, and the electromagnet on the other. Results of small prototype laboratory experiments are reported. The electromagnet has, for convenience, been replaced by a permanent SmCo ferromagnet in these measurements. When the two craft approach, a mirror image of the ferromagnet is induced in the Y123, and a repulsive bumper force, F_B, results. F_B is velocity dependent, and increases with v. For presently available HTS materials, bumper pressure of ~3.7N/cm^2 is achieved using SmCo. This extrapolates to ~18N/cm^2 for an electromagnet, or a force of up to 20 tons for a 1m^2 system. After reaching a minimum distance of approach, the two colliding craft begin to separate. However, the

consequent change of SmCo magnetic field at the Y123 results in a reversal of current in the Y123 so that the Y123 is attractive to the SmCo. The attractive (tether) force, F_T, is a function of $R=B_{Fe}/B_{t,max}$, where B_{Fe} is the field at the surface of the ferromagnet, and $B_{t,max}$ is the maximum trapped field of the Y123, i.e., the trapped field in the so-called critical state. For $R \geq 2$, F_T saturates at a value comparable to F_B. For a range of initial approach velocities the two craft are tethered following the bumper sequence. Most of the kinetic energy of the collision is first converted to magnetic field energy in the Y123, and then into heat via the creep mechanism. About 15% of the work done against magnetic forces during collision remains stored as magnetic energy after 1 hour. Experiments have also been conducted on the spatial range of the bumper force for arrays of HTS tiles. For a single HTS tile ~ 2cm in diameter, the range of F_B is ~ 1cm. For a $1m^2$ array the range of F_B will be circa 50 cm.

INTRODUCTION

Assume two spacecraft approach for docking. On one is an unactivated electromagnet and, facing this, on the other craft is an array of HTS tiles. As the craft near, the HTS is cooled in zero field (i.e., zero field cooled, or ZFC) and the electromagnet is then turned on. As the craft approach, the superconductor first acts like a mirror image of the approaching ferromagnet, and repels it. The Bean model [1] gives a good qualitative representation of the forces. The field of the ferromagnet, B_{Fe}, first induces current J_c in the outer parts of the superconductor. These penetrate to some interior point, r_{min}. At r_{min} the current goes to zero. The direction of this current is such that the two magnets repel. As B_{Fe} increases, r_{min} decreases, and reaches the center of the superconductor when $B_{Fe}=B_{t,max}$. Here $B_{t,max}$ is the maximum field which can be trapped in the HTS. The maximum bumper force, F_B, occurs for the ratio $R=B_{Fe}/B_{t,max} \leq 1$.

If the craft have momentum they will approach unless and until stopped by F_B. After the relative motion is stopped, the magnets continue to repel, and hence the craft develop velocity in the reverse direction. In this phase, B_{Fe} at the surface of the superconductor decreases. The resulting supercurrent in the HTS depends upon the value of the ratio $R \equiv B_{Fe}/B_{t,max}$ at the point of closest collision. For a range of values of R the dominant resulting supercurrent reverses, and force on the ferromagnet, due to the supercurrent, becomes attractive. This can lead to tethering, as will be discussed further below. The maximum tether force occurs for $R \geq 2$.

EXPERIMENTAL STUDY

Measurement of Bumper Force

A device was constructed to measure the forces acting in the HTS-SmCo system. This is shown schematically in Fig. 1. Transducers were used to measure quantities of interest, and direct computer logging was used. Initially, only force, and separation distance of the Fe-HTS were measured. The HTS used was $Y_{1.7}Ba_2Cu_3O_{7-\delta}$ (Y123). The size of the Y123 tiles used were ~ 2cm diameter and 0.8cm thick, except where it was desired to reduce $B_{t,max}$ in order to increase R. In these cases the 0.8cm thickness was reduced. The SmCo magnets used were comprised of one or more pieces, each of which was 1" x 1" x 1/4". By varying the number of SmCo pieces used, B_{Fe} could be varied from 2,000 to 4,300 Gauss.

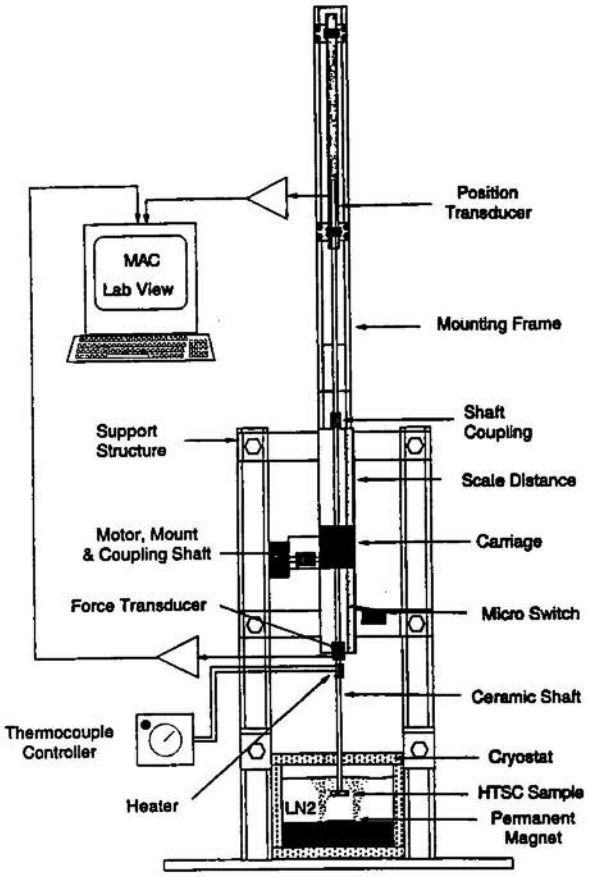

Fig. 1. Characterization apparatus for bumper/tether experiments.
Note: Transducers for magnetic field, temperature, and lateral forces have now been added to this device.

Figure 2 shows early measurements of the bumper force vs. distance in which it was learned that F_B depends upon the velocity of approach. This will be discussed below. The maximum values of F_B/Area observed were about 3.7N/cm^2. State-of-the-art HTS processing provides tiles of the size used for which $B_{t,max} \leq 2.1$Tesla.[2] However, the SmCo used was limited to about $B_{Fe} \sim 0.43$ Tesla. The maximum bumper force results from $B_{Fe}/B_{t,max} \sim 1$. Thus B_{Fe}, and not the HTS value of $B_{t,max}$, limited the magnitude of the bumper force when SmCo magnets were used. Electromagnets can be run, highly saturated, at up to $B_{Fe} \sim 2$

Tesla. Nevertheless, since $B_{t,max} \leq 2.1$ Tesla is available even today, the bumper force is limited by B_{Fe}, and not $B_{t,max}$ even when an electromagnet is used.

If we scale the results of the tests on our small prototype system to a system composed of HTS tiles with $B_{t,max} \geq 2.0$ Tesla, and $B_{Fe} \sim 2.0$ Tesla (for an electromagnet), then the bumper force scales to ~ 18.0N/cm^2. A system 1m^2 in size will exhibit bumper forces of $\geq$ 20 tons.

Velocity Dependence of Bumper Force

The HTS was zero field cooled (ZFC), and the force and work needed to bring the SmCo and HTS close together were measured. Repeated observations, such as presented in Fig. 2, made it clear that the bumper force, F_B, was velocity dependent. In this experiment, involving one tile of Y123, and one small SmCo magnet, the largest velocity of approach permitted by the specific equipment used was ~ 1m/sec. At this velocity, F_B was about 11N. In order to study the velocity dependence of the bumper force, the test apparatus was developed further to include motor drives of constant velocity. This study of F_B indicated that the dominant cause of the velocity dependency is the "giant creep" phenomenon. The creep effect describes a loss of magnetic field by a high temperature superconductor, after initial activation. In the creep mechanism, if the HTS trapped field B_t (t_1) is

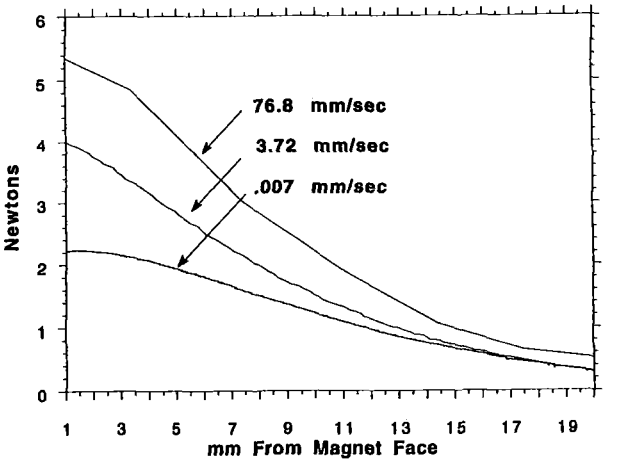

Fig. 2. Bumper force, in N, vs. separation of ferromagnet and HTS, in mm, with velocity of approach as a parameter. For this experiment a motor drive was added to the apparatus.

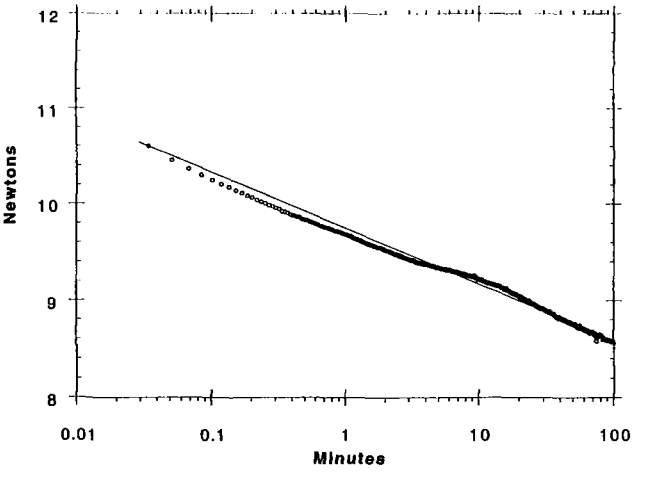

Fig. 3. Effect of creep on bumper force. The SmCo-HTS separation distance was closed rapidly. Following this F_B vs. time was observed.

measured at some time t_1, than at some later time, t_2,

$$B_t(t_2) = B_t(t_1)(1-\beta_1 \log(t_2-t_1)) \quad (1)$$

The creep rate for the materials and tile sizes used in this experiment have been measured repeatedly [3,4]. For a wide variety of processes and sizes, they are characterized in Eq. 1 by a value,

$$0.045 \leq \beta_1 \leq 0.055 \quad (2)$$

i.e., as a rule of thumb the trapped field in a tile of Y123 decreases at ~5% per decade of time.

In order to directly observe the creep effect on the bumper force, the maximum velocity available to us was used, and the Fe/HTS separation gap was closed to a very small separation in a few hundredths of a second. The separation was then left constant. The resulting force, as a function of time following the collision is shown in Fig 3.

The data of Fig. 3 is a good fit to

$$F(t_2) = F(t_1)(1-\beta_2 \log(t_2 - t_1)) \quad (3)$$

with

$$\beta_2 \sim 0.055 \quad (4)$$

This is as expected for a force proportional to ∇B_t, and hence to B_t.

At low collision velocities the field induced in the HTS is reduced by creep. At high velocities there is insufficient time for this, and hence a greater induced field results in the HTS, which in turn results in a larger value of F_B.

Energy Considerations

Our group earlier developed a model of the currents which flow in an HTS trapped field magnet [5]. The model describes the current as composed of two parts: (i) a volume current of constant current density, circulating around the field direction, as would a Bean current [1], and (ii) a constant surface current density on the outer periphery of the HTS, similar to an Amperian current density in a

ferromagnet. This current model provides excellent fits to the three dimensional field around trapped field HTS magnets.

The current model thus permits calculating trapped field energies. Using the current model [5], and a few points of measured trapped field, the magnetic field can be calculated for all space. From this the magnetic energy density can be calculated and then integrated. Typically, in these experiments, we found that 15% of the work done in the collision was still stored as magnetic energy in the HTS an hour after the collision.

In principle one can use such a measurement and calculation of stored energy, together with the creep equation (Eq. 1), to calculate the energy stored in the magnetic field of the HTS as a function of time. The creep rate, β, of Eq. 1 is both measured in this experiment, and known from previous work [Refs 3,4] for the time interval 1sec < t < 1 year. However, the creep rate for short times, t << 1 sec, is not available from our own measurements. Such data is available in the literature, and indicate a faster creep speed at very short times [6].

We used the measured creep, as shown in Fig. 3, and the measurement by others of creep at very short times, and concluded that most, if not all, of the kinetic energy lost in the collision is converted to magnetic field energy in the HTS. The magnetic energy is then converted to heat at a rate given by the creep mechanism.

The Bounce Back

After closest approach, the SmCo is repelled, by the HTS, and the separation increases. The nature of the Bean current [1] is such that the decreasing SmCo field results in a reversal of current in the outer regions of the HTS. The size of the region of reversal depends on the ratio $R = B_{Fe}/B_{t,max}$. For values of R of the order of 1, or larger, the repelling force reverses, and becomes an attractive force at a small separation distance. This can result in trapping the HTS and SmCo magnets close to each other, but not touching. The tether force depends upon the ratio $B_{Fe}/B_{t,max}$. See Figure 4. The tether force becomes maximum when $B_{Fe} \geq 2B_{t,max}$. This is also explained by the Bean model [1] which predicts that as the ferromagnet retreats, and B_{Fe} decreases at the surface of the HTS, J_c reverses, and an attractive field and force results, which is maximum when B_{Fe} is at least twice $B_{t,max}$.

Again we note that J_c, and B_t, for state-of-the-art HTS are quite sufficient for the HTS role in the device described here. Typical maximum trapped fields in our HTS tiles at 77K are 0.4-0.5 Tesla when not irradiated, 1.1 to 1.2 Tesla when proton irradiated [8] and 2.1 Tesla when processed with short isotropic columnar defects [7, 2]. $B_{t,max}$ had to be *reduced,* even in our unirradiated tiles, to observe cases in which the maximum tether force occurred. Thus the HTS used to observe tethering was not irradiated, and for some measurements the HTS tiles were thinned.

Fig. 5 shows the work done against F_B, in the movement toward closest approach, and by F_T in the retreat from closest approach. Fig 5 uses as input data the forces shown in Fig. 4c. In this example, the craft approach and their kinetic energy is gradually reduced by F_B, until the kinetic energy reaches zero at the distance of closest approach. Then F_T at first causes an acceleration in the opposite direction. However, when the craft reach point (a), in their retreat, F_T reverses and slows the retreat. The craft become energetically trapped in the region between (b) and the distance of closest approach. The craft will oscillate in this interval until dissipative forces bring them to rest at point (a).

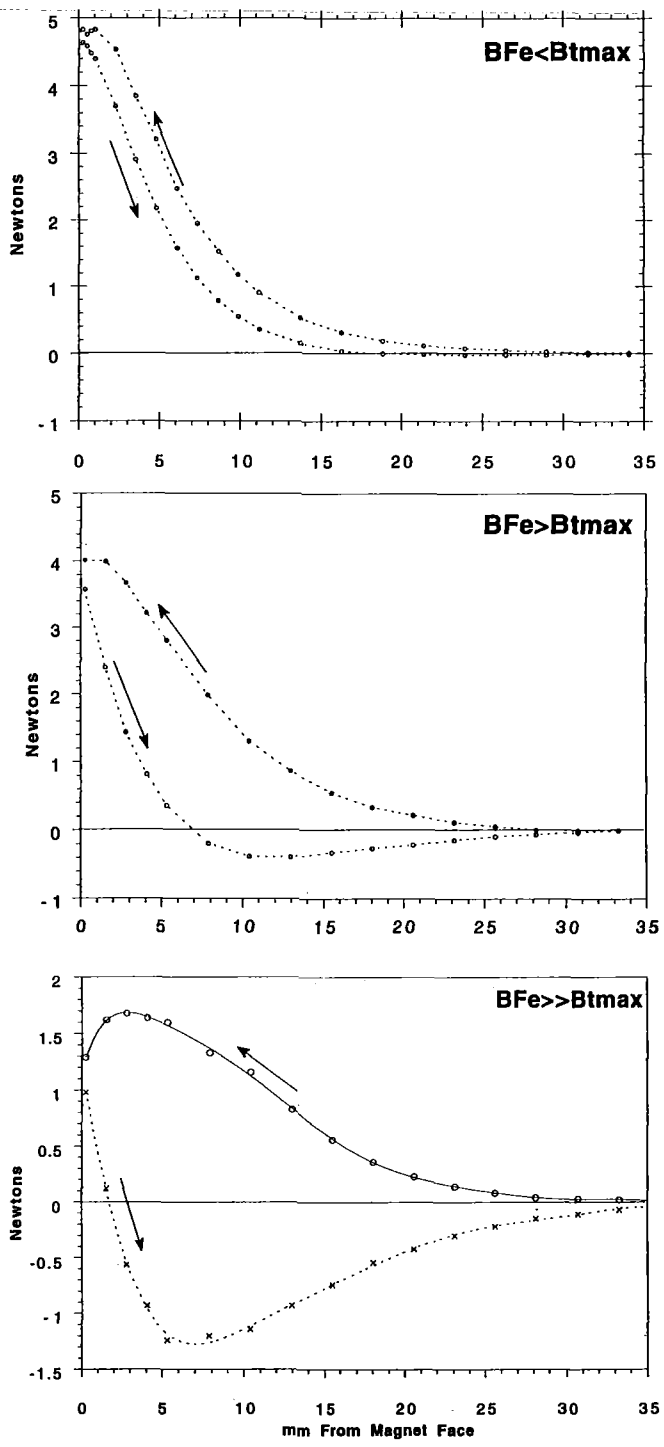

Fig. 4. F_B (arrow to left), and F_T (arrow to right) are shown for $R \equiv B_{Fe}/B_{t,max} = 0.67$ (top); 1.39 (middle); and 2.47 (bottom).

Range of the Magnetic Forces

The range of the bumper force, F_B, is about equal to the radius of the tile of HTS material. Most high quality HTS tiles have radius of 1-3 cm. Thus the range of F_B, for a single HTS tile, is 1-3 cm. (See Figure 4a.) Bumper operation can be useful at 1-3 cm as a backup for more traditional docking mechanisms in spacecraft. However, it would clearly be desirable to extend the range of the bumper force.

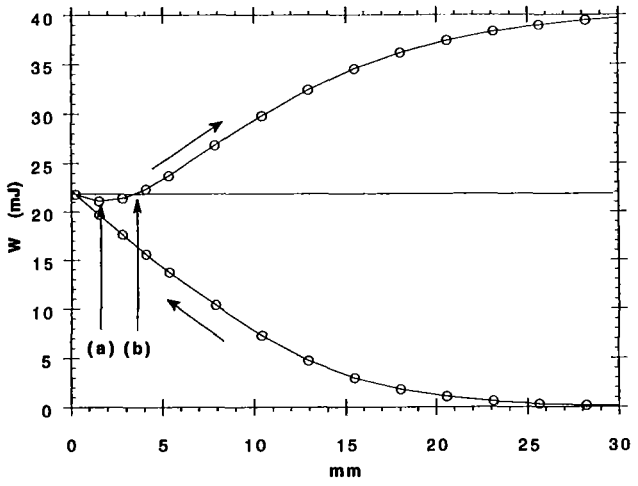

Fig. 5. Work done by spacecraft on magnetic field, in case of forces shown in Fig. 4c. On approach (arrow to right) spacecraft do work of 22mJ. At distance of closest approach, KE = 0. On bounce back spacecraft cannot separate beyond point (b).

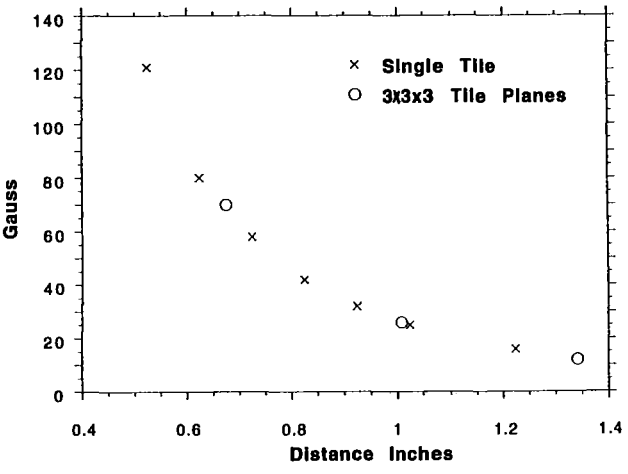

Fig. 6. Evidence for scaling, comparing trapped field of a single tile at distance Z from surface, to trapped field of an array of 3 x 3 x 3 tiles at a distance 3 x Z.

We have performed experiments to determine the scaling laws for *arrays* of HTS tiles. For these purposes we have used an array of 3 x 3 x 3 HTS tiles, and arrays of 1 x 5 x 5 and 2 x 5 x 5 tiles.

A single tile of HTS, of radius r_0, has a range of the order of r_0. One theoretically expects that an array of n x n x n HTS tiles will have a range of the order of n x r_0. This expectation has been confirmed experimentally for the 3 x 3 x 3 array of tiles. See Figure 6. Comparable extension of field range has been observed in 5 x 5 x 1 and 5 x 5 x 2 arrays. We expect therefore that an array of 50 x 50 tiles (of total size about 1m x 1m) will have a field range of about 50cm.

SUMMARY

A magnetic bumper-tether has been explored using 2cm diameter, 0.8 cm thick HTS tiles, ZFC, and similar size SmCo ferromagnets. Bumper forces, F_B, are observed up to $F_B \sim 11N$. F_B of the order of 20 tons can be achieved for arrays of the order of 1m x 1m for HTS tiles, used with an electromagnet. Because of creep, the bumper force is velocity dependent, having its highest values for the largest approach velocity, as is desirable. The bumper force maximizes for $R \equiv B_{Fe}/B_{t,max} \leq 1$.

The tether force, F_T, is comparable to the bumper force when $R \geq 2$. The tether force leads to automatic tethering for a range of values of R.

Bumper and tether forces, combined, will optimize in the interval $1 \leq R \leq 2$.

During the collision most of the mechanical work done in the collision is converted to magnetic field energy, and then to heat via the creep mechanism. One hour after the collision, 15% of the energy remains in the magnetic field.

The range of the bumper force for a single tile is only ~ 1cm. However the range of the force increases with the size of the total array of HTS tiles, and reaches, ~ 50 cm for an array of tiles 1m x 1m.

Work on this project continues, to determine the lateral stability of the bumper cycle, to test larger prototypes using arrays, and to make large-scale prototype collision tests. The theory of the dependence of F_B and F_T on R is being more fully developed. The present test device is being extended by adding magnetic field and temperature transducers, and force transducers to measure lateral forces.

This work was supported by NASA-JSC, NSF, ARO, and the State of Texas via TCSUH and the ATP Program.

REFERENCES

1. Bean, C.P.; Phys. Rev. Lett., 8, 250 (1962); Rev. Mod. Phys., 36, 31 (1964)

2. Weinstein, R.; Sawh, R.-P.; Ren, Y.; and Liu, J.: "The Effect of Isotropic Short Columnar Pinning Centers on J_c, T_c, and Creep," submitted to Eighth International Workshop on Critical Currents in Superconductors, Kitakyushu, Japan, April 1996.
3. Weinstein, R.; Ren, Y.; Liu J.; Chen, I.G.; Sawh, R.; Foster, C.; and Obot, V.; Proc. Intl. Symposium on Superconductivity, Vol 2, pg 855, Hiroshima, Springer Verlag (1993)
4. Weinstein, R.; Chen, I.G.; Liu, J.; Parks, D.; Selvamanickam, V.; and Salama, K.; Appl. Phys. Lett., 56, 1475 (1990)
5. Liu, J.; Chen, I.G.; Weinstein, R.; and Xu, J.; Jour. Appl. Phys., 73, 6530 (1993); Chen, I.G.; Liu, J.; Weinstein, R.; and Lau, K.; Jour. Appl. Phys., 72, 1013 (1992)
6. Gao, L.; Xue, Y.; Hor, P.; and Chu, C.W., Physica, C177, 438 (1991)
7. Weinstein, R.; et al, Invited Paper, Proc. International Workshop on Superconductivity, Kyoto, Japan (June 1994)
8. Weinstein, R.; Ren, Y.; Liu, J.; Sawh, R.; Parks, D.; Foster, C.; Obot, V.; Arndt, G.D.; and Crapo, A.; Proc. of Fourth World Congress on Superconductivity, Vol. I, pg. 158, Orlando (1994).